

FIXED-ORDER H-INFINITY CONTROL FOR INTERCONNECTED SYSTEMS USING DELAY DIFFERENTIAL ALGEBRAIC EQUATIONS

SUAT GUMUSSOY AND WIM MICHIELS*

Abstract. We analyze and design H-infinity controllers for general time-delay systems with time-delays in systems' state, inputs and outputs. We allow the designer to choose the order of the controller and to introduce constant time-delays in the controller. The closed-loop system of the plant and the controller is modeled by a system of delay differential algebraic equations (DDAEs). The advantage of the DDAE modeling framework is that any interconnection of systems and controllers prone to various types of delays can be dealt with in a systematic way, without using any elimination technique. We present a predictor-correct algorithm for the H-infinity norm computation of systems described by DDAEs. Instrumental to this we analyze the properties of the H-infinity norm. In particular, we illustrate that it may be sensitive with respect to arbitrarily small delay perturbations. Due to this sensitivity, we introduce the strong H-infinity norm which explicitly takes into account small delay perturbations, inevitable in any practical control application. We present a numerical algorithm to compute the strong H-infinity norm for DDAEs. Using this algorithm and the computation of the gradient of the strong H-infinity norm with respect to the controller parameters, we minimize the strong H-infinity norm of the closed-loop system based on non-smooth, non-convex optimization methods. By this approach, we tune the controller parameters and design H-infinity controllers with a prescribed order or structure.

1. Introduction. In many control applications, robust controllers are desired to achieve stability and performance requirements under model uncertainties and exogenous disturbances [35]. The design requirements are usually defined in terms of \mathcal{H}_∞ norms of closed-loop transfer functions including the plant, the controller and weights for uncertainties and disturbances. There are robust control methods to design the optimal \mathcal{H}_∞ controller for linear finite dimensional multi-input-multi-output (MIMO) systems based on Riccati equations and linear matrix inequalities (LMIs), see e.g. [9, 16] and the references therein. The order of the controller designed by these methods is typically larger or equal then the order of the plant. This is a restrictive condition for high-order plants, since low-order controllers are desired in a practical implementation. The design of fixed-order or low-order \mathcal{H}_∞ controller can be translated into a non-smooth, non-convex optimization problem. Recently fixed-order \mathcal{H}_∞ controllers have been successfully designed for finite dimensional linear-time-invariant (LTI) MIMO plants using a direct optimization approach [20]. This approach allows the user to choose the controller order and tunes the parameters of the controller to minimize the \mathcal{H}_∞ norm under consideration. An extension to a class of retarded time-delay systems has been described in [18].

In this work we design a fixed-order or fixed-structure \mathcal{H}_∞ controller in a feedback connection with a time-delay system. The closed-loop system is a delay differential algebraic system and its state-space representation is written as

$$\begin{cases} E\dot{x}(t) = A_0x(t) + \sum_{i=1}^m A_ix(t - \tau_i) + Bw(t), \\ z(t) = Cx(t). \end{cases} \quad (1.1)$$

The time-delays τ_i , $i = 1, \dots, m$ are positive real numbers and the capital letters are real-valued matrices with appropriate dimensions. The input w and output z are disturbances and signals to be minimized to achieve design requirements and some of the system matrices include the controller parameters.

*Department of Computer Science, Katholieke Universiteit Leuven, Belgium, (`{Suat.Gumussoy,Wim.Michiels}@cs.kuleuven.be`)

The system with the closed-loop equations (1.1) represents all interesting cases of the feedback connection of a time-delay plant and a controller. The transformation of the closed-loop system to this form can be easily done by first augmenting the system equations of the plant and controller. As we shall see, this augmented system can subsequently be brought in the form (1.1) by introducing slack variables to eliminate input/output delays and direct feedthrough terms in the closed-loop equations. Hence, the resulting system of the form (1.1) is obtained directly without complicated elimination techniques that may even not be possible in the presence of time-delays.

As we shall see, the \mathcal{H}_∞ norm of DDAEs may be sensitive to arbitrarily small delay changes. Since small modeling errors are inevitable in any practical design we are interested in the smallest upper bound of the \mathcal{H}_∞ norm that is insensitive to small delay changes. Inspired by the concept of strong stability of neutral equations [21], this leads us to the introduction of the concept of *strong \mathcal{H}_∞ norms* for DDAEs. Several properties of the strong \mathcal{H}_∞ norm are shown and a computational formula is obtained. The theory derived can be considered as the dual of the theory of strong stability as elaborated in [11, 21, 23, 24, 28, 30] and the references therein.

In addition, a level set algorithm for computing strong \mathcal{H}_∞ norms is presented. Level set methods rely on the property that the frequencies at which a singular value of the transfer function equals a given value (the level) can be directly obtained from the solutions of a linear eigenvalue problem with Hamiltonian symmetry (see, e.g. [1, 2, 5, 7]), allowing a two-directional search for the global maximum. For time-delay systems this eigenvalue problem is infinite-dimensional. Therefore, we adopt a predictor-corrector approach, where the prediction step involves a finite-dimensional approximation of the problem, and the correction serves to remove the effect of the discretization error on the numerical result. The algorithm is inspired by the algorithm for \mathcal{H}_∞ computation for time-delay systems of retarded type as described in [25]. However, a main difference lies in the fact that the robustness w.r.t. small delay perturbations needs to be explicitly addressed.

The numerical algorithm for the norm computation is subsequently applied to the design of \mathcal{H}_∞ controllers by a direct optimization approach. In the context of control of LTI systems it is well known that \mathcal{H}_∞ norms are in general non-convex functions of the controller parameters which arise as elements of the closed-loop system matrices. They are typically even not everywhere smooth, although they are differentiable almost everywhere [20]. These properties carry over to the case of strong \mathcal{H}_∞ norms of DDAEs under consideration. Therefore, special optimization methods for non-smooth, non-convex problems are required. We will use a combination of BFGS, whose favorable properties in the context of non-smooth problems have been reported in [22], bundle and gradient sampling methods, as implemented in the MATLAB code HANSO¹. The overall algorithm only requires the evaluation of the objective function, i.e., the strong \mathcal{H}_∞ norm, as well as its derivatives with respect to the controller parameters whenever it is differentiable. The computation of the derivatives is also discussed in the paper.

The presented method is frequency domain based and builds on the eigenvalue based framework developed in [26]. Time-domain methods for the \mathcal{H}_∞ control of DDAEs have been described in [15] and the references therein, based on the construction of Lyapunov-Krasovskii functionals.

The structure of the article is as follows. In Section 2 we illustrate the generality

¹Hybrid Algorithm for Nonsmooth Optimization, see [33]

of the system description (1.1). Preliminaries and assumptions are given in Section 3. The definition and properties of the strong \mathcal{H}_∞ norm of DDAE are given in Section 4. The numerical algorithm to compute the strong \mathcal{H}_∞ norm is described in detail in Section 5. Fixed-order \mathcal{H}_∞ controller design is addressed in Section 6. Section 7 is devoted to the numerical examples. In Section 8 some concluding remarks are presented. Some technical lemmas and finite dimensional approximation of time-delay systems are given in Appendices A and B respectively.

Notations. The notations are as follows:

j	: the imaginary unit
\mathbb{C}, \mathbb{R}	: set of the complex and real numbers
\mathbb{N}	: set of natural numbers
$\mathbb{R}^+, \mathbb{R}_0^+$: set of nonnegative and strictly positive real numbers
A^*	: complex conjugate transpose of the matrix A
A^{-T}	: transpose of the inverse matrix of A
A^\perp	: matrix of full column rank whose columns span the orthogonal complement of A
I, I_n	: identity matrix of appropriate dimensions, of dimensions $n \times n$
$0, 0_n, 0_{n \times m}$: zero matrix with appropriate dimensions, with dimension $n \times n$, with dimensions $n \times m$
$\sigma_i(A)$: i^{th} singular value of A , $\sigma_1(\cdot) \geq \sigma_2(\cdot) \geq \dots$
$\Re(u)$: real part of the complex number u
$\Im(u)$: imaginary part of the complex number u
$\mathcal{D}(\cdot)$: domain of an operator
$\mathcal{C}, \mathcal{L}_2$: the space of continuous and square integrable complex functions, i.e., $\mathcal{L}_2([-\tau_{\max}, 0], \mathbb{C}^n) := \{f : [-\tau_{\max}, 0] \rightarrow \mathbb{C}^n : \int_{-\tau_{\max}}^0 f(t) ^2 dt < \infty\}$
$\vec{\tau} \in \mathbb{R}^m$: short notation for (τ_1, \dots, τ_m)
$\mathcal{B}(\vec{\tau}, \epsilon)$: open ball of radius $\epsilon \in \mathbb{R}^+$ centered at $\vec{\tau} \in (\mathbb{R}^+)^m$, $\mathcal{B}(\vec{\tau}, \epsilon) := \{\vec{\theta} \in (\mathbb{R})^m : \ \vec{\theta} - \vec{\tau}\ < \epsilon\}$
$\left[\begin{array}{c c} A & B \\ \hline C & D \end{array} \right]$: transfer function representation for $T(\lambda) = C(\lambda I - A)^{-1}B + D$

2. Motivating examples. With some simple examples we illustrate the generality of the system description (1.1).

EXAMPLE 2.1. Consider the feedback interconnection of the system

$$\begin{cases} \dot{x}(t) &= Ax(t) + B_1 u(t) + B_2 w(t), \\ y(t) &= Cx(t) + D_1 u(t), \\ z(t) &= Fx(t), \end{cases}$$

and the controller

$$u(t) = Ky(t - \tau).$$

For $\tau = 0$ it is possible to eliminate the output and controller equation, which results in the closed-loop system

$$\begin{cases} \dot{x}(t) &= Ax(t) + B_1 K(I - D_1 K)^{-1} Cx(t) + B_2 w(t), \\ z(t) &= Fx(t). \end{cases} \quad (2.1)$$

This approach is for instance taken in the software package HIFOO [6]. If $\tau \neq 0$, then the elimination is not possible any more. However, if we let $X = [x^T \ u^T \ y^T]^T$ we can

describe the system by the equations

$$\begin{cases} \begin{bmatrix} I & 0 & 0 \\ 0 & 0 & 0 \\ 0 & 0 & 0 \end{bmatrix} \dot{X}(t) = \begin{bmatrix} A & B_1 & 0 \\ C & D_1 & -I \\ 0 & I & 0 \end{bmatrix} X(t) - \begin{bmatrix} 0 & 0 & 0 \\ 0 & 0 & 0 \\ 0 & 0 & K \end{bmatrix} X(t - \tau) + \begin{bmatrix} B_2 \\ 0 \\ 0 \end{bmatrix} w(t), \\ z(t) = \begin{bmatrix} F & 0 & 0 \end{bmatrix} X(t), \end{cases}$$

which are of the form (1.1). Furthermore, the dependence of the matrices of the closed-loop system on the controller parameters, K , is still linear, unlike in (2.1).

EXAMPLE 2.2. The presence of a direct feedthrough term from w to z , as in

$$\begin{cases} \dot{x}(t) &= Ax(t) + A_1x(t - \tau) + Bw(t), \\ z(t) &= Fx(t) + D_2w(t), \end{cases} \quad (2.2)$$

can be avoided by introducing a slack variable. If we let $X = [x^T \ \gamma_w^T]^T$, where γ_w is the slack variable, we can bring (2.2) in the form (1.1):

$$\begin{cases} \begin{bmatrix} I & 0 \\ 0 & 0 \end{bmatrix} \dot{X}(t) = \begin{bmatrix} A & 0 \\ 0 & -I \end{bmatrix} X(t) + \begin{bmatrix} A_1 & 0 \\ 0 & 0 \end{bmatrix} X(t - \tau) + \begin{bmatrix} B \\ I \end{bmatrix} w(t), \\ z(t) = \begin{bmatrix} F & D_2 \end{bmatrix} X(t). \end{cases}$$

EXAMPLE 2.3. The system

$$\begin{cases} \dot{x}(t) &= Ax(t) + B_1w(t) + B_2w(t - \tau), \\ z(t) &= Cx(t), \end{cases}$$

can also be brought in the standard form (1.1) by a slack variable. Letting $X = [x^T \ \gamma_w^T]^T$ we can express

$$\begin{cases} \dot{X}(t) &= \begin{bmatrix} A & B_1 \\ 0 & -I \end{bmatrix} X(t) + \begin{bmatrix} 0 & B_2 \\ 0 & 0 \end{bmatrix} X(t - \tau) + \begin{bmatrix} 0 \\ I \end{bmatrix} w(t), \\ z(t) &= \begin{bmatrix} C & 0 \end{bmatrix} X(t). \end{cases}$$

In a similar way one can deal with delays in the output z .

Using the techniques illustrated with the above examples a broad class of interconnected systems with delays can be brought in the form (1.1), where the external inputs w and outputs z stem from the performance specifications expressed in terms of appropriately defined transfer functions. As a more realistic illustration, the feed-back interconnection of any retarded type time-delay system G and controller K with the following state-space representations,

$$G : \begin{cases} \dot{x}_G(t) = \sum_{i=0}^{m_a} A^i x_G(t - \tau_i^a) + \sum_{i=0}^{m_{b1}} B_1^i w(t - \tau_i^{b1}) + \sum_{i=0}^{m_{b2}} B_2^i u(t - \tau_i^{b2}) \\ z(t) = \sum_{i=0}^{m_{c1}} C_1^i x_G(t - \tau_i^{c1}) + \sum_{i=0}^{m_{d11}} D_{11}^i w(t - \tau_i^{d11}) + \sum_{i=0}^{m_{d12}} D_{12}^i u(t - \tau_i^{d12}) \\ y(t) = \sum_{i=0}^{m_{c2}} C_2^i x_G(t - \tau_i^{c2}) + \sum_{i=0}^{m_{d21}} D_{21}^i w(t - \tau_i^{d21}) + \sum_{i=0}^{m_{d22}} D_{22}^i u(t - \tau_i^{d22}), \end{cases} \quad (2.3)$$

$$K : \begin{cases} \dot{x}_K(t) = \sum_{i=0}^{m_{a_k}} A_K^i x_K(t - \tau_i^{a_k}) + \sum_{i=0}^{m_{b_k}} B_K^i y(t - \tau_i^{b_k}) \\ u(t) = \sum_{i=0}^{m_{c_k}} C_K^i x_K(t - \tau_i^{c_k}) + \sum_{i=0}^{m_{d_k}} D_K^i u(t - \tau_i^{d_k}), \end{cases} \quad (2.4)$$

can be written in the form of (1.1) using similar techniques in the previous examples.

The price to pay for the generality of the framework is the increase of the dimension of the system, n , which affects the efficiency of the numerical methods. However, this is a minor problem in most applications because the delay difference equations or algebraic constraints are related to inputs and outputs, and the number of inputs and outputs is usually much smaller than the number of state variables.

3. Preliminaries.

Assumptions. Let $\text{rank}(E) = n - \nu$, with $\nu \leq n$, and let the columns of matrix $U \in \mathbb{R}^{n \times \nu}$, respectively $V \in \mathbb{R}^{n \times \nu}$, be a (minimal) basis for the left, respectively right nullspace, that is,

$$U^T E = 0, \quad EV = 0.$$

Throughout the paper we make the following assumption.

ASSUMPTION 3.1. *The matrix $U^T A_0 V$ is nonsingular.*

In order to motivate Assumption 3.1, we note that the equations (1.1) can be separated into coupled delay differential and delay difference equations. When we define

$$\mathbf{U} = [U^\perp \ U], \quad \mathbf{V} = [V^\perp \ V],$$

a pre-multiplication of (1.1) with \mathbf{U}^T and the substitution

$$x = \mathbf{V} [x_1^T \ x_2^T]^T,$$

with $x_1(t) \in \mathbb{R}^{n-\nu}$ and $x_2(t) \in \mathbb{R}^\nu$, yield the coupled equations

$$\begin{cases} E^{(11)} \dot{x}_1(t) &= \sum_{i=0}^m A_i^{(11)} x_1(t - \tau_i) + \sum_{i=0}^m A_i^{(12)} x_2(t - \tau_i) + B_1 w(t), \\ 0 &= A_0^{(22)} x_2(t) + \sum_{i=1}^m A_i^{(22)} x_2(t - \tau_i) \\ &\quad + \sum_{i=0}^m A_i^{(21)} x_1(t - \tau_i) + B_2 w(t), \\ z(t) &= C_1 x_1(t) + C_2 x_2(t), \end{cases} \quad (3.1)$$

where

$$\begin{aligned} A_i^{(11)} &= U^{\perp T} A_i V^\perp, & A_i^{(12)} &= U^{\perp T} A_i V, \\ A_i^{(21)} &= U^T A_i V^\perp, & A_i^{(22)} &= U^T A_i V, \quad i = 0, \dots, m, \end{aligned}$$

and

$$E^{(11)} = U^{\perp T} E V^\perp, \quad B_1 = U^{\perp T} B, \quad B_2 = U^T B, \quad C_1 = C V^\perp, \quad C_2 = C V.$$

Matrix $E^{(11)}$ in (3.1) is invertible, following from

$$n - \nu = \text{rank}(E) = \text{rank}(\mathbf{U}^T E \mathbf{V}) = \text{rank}(E^{(11)}).$$

In addition, matrix $A_0^{(22)}$ is invertible, following from Assumption 3.1.

The equations (3.1), with $w \equiv 0$, are semi-explicit delay differential algebraic equations of index 1, because delay differential equations are obtained by differentiating the second equation. This precludes the occurrence of impulsive solutions [15]. Moreover, the invertibility of $A_0^{(22)}$ prevents that the equations are of *advanced* type and, hence, non-causal. This further motivates why Assumption 3.1 is natural in the delay case considered, although it restricts the index to one (for a general treatment in the delay free case, see for instance [34] and the references therein).

We further make the following assumption.

ASSUMPTION 3.2. *The zero solution of system (1.1), with $w \equiv 0$, is strongly exponentially stable.*

Strong exponential stability refers to the fact that the asymptotic stability of the null solution is robust against small delay perturbations [21, 30]. Due to modeling errors and uncertainty, the delays in the model are usually not exact and this type of stability is required in practice. The stability of the closed-loop system (1.1) is a necessary assumption for \mathcal{H}_∞ norm optimization since this norm is finite for stable systems only. We assume that parameters of a controller are available such that the closed-loop system of the form (1.1) is strongly exponentially stable. These parameters can, for instance, be found by minimizing the spectral abscissa of the closed-loop system (1.1) using a non-smooth, non-convex optimization method [20]. The overall \mathcal{H}_∞ optimization of the closed-loop system (1.1) can then be performed in two steps. First a fixed-order or fixed-structure controller strongly stabilizing the closed-loop system (1.1) is designed. Next the controller parameters are tuned to minimize the \mathcal{H}_∞ norm of the closed-loop system (1.1) starting from the initial controller obtained in the first step. In this article we focus on the \mathcal{H}_∞ computation and optimization.

Transfer functions. From (3.1) we can write the transfer function of the system (1.1) as

$$T(\lambda) := C \left(\lambda E - A_0 - \sum_{i=1}^m A_i e^{-\lambda \tau_i} \right)^{-1} B, \quad (3.2)$$

$$= [C_1 \ C_2] \begin{bmatrix} \lambda E^{(11)} - A_{11}(\lambda) & -A_{12}(\lambda) \\ -A_{21}(\lambda) & -A_{22}(\lambda) \end{bmatrix}^{-1} \begin{bmatrix} B_1 \\ B_2 \end{bmatrix}, \quad (3.3)$$

with

$$A_{kl}(\lambda) = \sum_{i=0}^m A_i^{(kl)} e^{-\lambda \tau_i}, \quad k, l \in \{1, 2\}.$$

The *asymptotic* transfer function of the system (1.1) is defined as

$$\begin{aligned} T_a(\lambda) &:= -CV \left(U^T A_0 V + \sum_{i=1}^m U^T A_i V e^{-\lambda \tau_i} \right)^{-1} U^T B \\ &= -C_2 A_{22}(\lambda)^{-1} B_2. \end{aligned} \quad (3.4)$$

The terminology stems from the fact that the transfer function T and the asymptotic transfer function T_a converge to each other for high frequencies. This is precisely stated in the following Proposition.

PROPOSITION 3.3. $\forall \gamma > 0, \exists \Omega > 0: \sigma_1(T(j\omega) - T_a(j\omega)) < \gamma, \forall \omega > \Omega.$

Proof. The assertion follows from the explicit expression for the inverse of the two-by-two block matrix in (3.3), combined with the property that

$$\sup_{\Re(\lambda) \geq 0} \left\| (A_{22}(\lambda))^{-1} \right\|_2 \quad (3.5)$$

is finite. The latter is due to Assumption 3.2. \square

The \mathcal{H}_∞ norm of the transfer function T of the *stable* system (1.1), is defined as

$$\|T(j\omega)\|_\infty := \sup_{\omega \in \mathbb{R}} \sigma_1(T(j\omega)).$$

Similarly we can define \mathcal{H}_∞ norm of T_a .

4. The strong \mathcal{H}_∞ norm of time-delay systems. We now analyze continuity properties of the \mathcal{H}_∞ norm of the transfer function T with respect to the delay parameters. The function

$$\vec{\tau} \in (\mathbb{R}_0^+)^m \mapsto \|T(j\omega, \vec{\tau})\|_\infty \quad (4.1)$$

is, in general, not continuous, which is inherited from the behavior of the asymptotic transfer function, T_a , more precisely the function

$$\vec{\tau} \in (\mathbb{R}_0^+)^m \mapsto \|T_a(j\omega, \vec{\tau})\|_\infty. \quad (4.2)$$

We start with a motivating example

EXAMPLE 4.1. *Let the transfer function T be defined as*

$$T(\lambda, \vec{\tau}) = \frac{\lambda + 2.1}{(\lambda + 0.1)(1 - 0.25e^{-\lambda\tau_1} + 0.5e^{-\lambda\tau_2}) + 1} \quad (4.3)$$

where $(\tau_1, \tau_2) = (1, 2)$. The transfer function T is stable, its \mathcal{H}_∞ norm is 2.5788, achieved at $\omega = 1.6555$ and the maximum singular value plot is given in Figure 4.1. The high frequency behavior is described by the asymptotic transfer function

$$T_a(\lambda, \vec{\tau}) = \frac{1}{(1 - 0.25e^{-\lambda\tau_1} + 0.5e^{-\lambda\tau_2})}, \quad (4.4)$$

whose \mathcal{H}_∞ norm is equal to 2.0320, which is less than $\|T(j\omega, \vec{\tau})\|_\infty$. However, when the first time delay is perturbed to $\tau_1 = 0.99$, the \mathcal{H}_∞ norm of the transfer function T is 3.9993, reached at $\omega = 158.6569$, see Figure 4.2. The \mathcal{H}_∞ norm of T is quite different from that for $(\tau_1, \tau_2) = (1, 2)$. A closer look at the maximum singular value plot of the asymptotic transfer function T_a in Figure 4.3 shows that the sensitivity is due to the transfer function T_a .

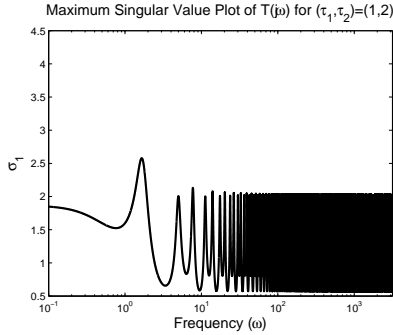


FIG. 4.1. The maximum singular value plot of $T(j\omega, \vec{\tau})$ for $(\tau_1, \tau_2) = (1, 2)$ as a function of ω .

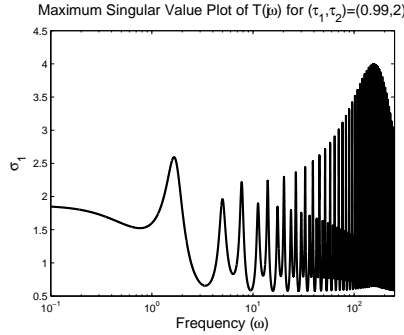


FIG. 4.2. The maximum singular value plot of $T(j\omega, \vec{\tau})$ for $(\tau_1, \tau_2) = (0.99, 2)$ as a function of ω .

Even if the first delay is perturbed slightly to $\tau_1 = 0.999$, the problem is not resolved, indicating that the functions (4.1) and (4.2) are discontinuous at $(\tau_1, \tau_2) = (1, 2)$. The \mathcal{H}_∞ norm of the transfer function T for $(\tau_1, \tau_2) = (0.999, 2)$ is given by 3.9944, and the peak value is reached at $\omega = 1515.8091$. The corresponding asymptotic transfer function T_a is shown in Figure 4.4. When the delay perturbation tends to zero, the frequency where the maximum in the singular value plot of the asymptotic transfer function T_a is achieved moves towards infinity.

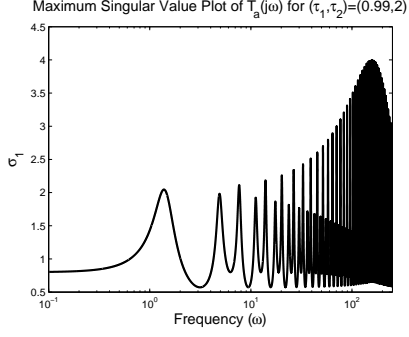


FIG. 4.3. The maximum singular value plot of $T_a(j\omega, \vec{\tau})$ for $(\tau_1, \tau_2) = (0.99, 2)$ as a function of ω .

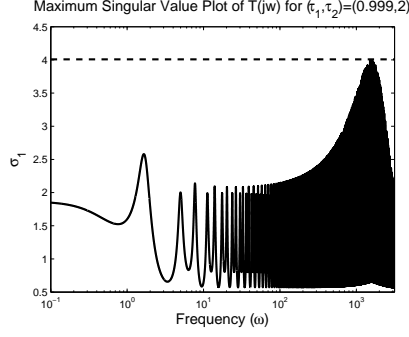


FIG. 4.4. The maximum singular value plot of $T_a(j\omega, \vec{\tau})$ for $(\tau_1, \tau_2) = (0.999, 2)$ as a function of ω .

The above example illustrates that the \mathcal{H}_∞ norm of the transfer function T may be sensitive to *infinitesimal* delay changes. On the other hand, for any $\omega_{\max} > 0$, the function

$$\vec{\tau} \mapsto \max_{[0, \omega_{\max}]} \sigma_1(T(j\omega, \vec{\tau})),$$

where the maximum is taken over a compact set, is continuous, because a discontinuity would be in contradiction with the continuity of the maximum singular value function of a matrix. Hence, the sensitivity of the \mathcal{H}_∞ norm is related to the behavior of the transfer function at high frequencies and, hence, the asymptotic transfer function T_a . Accordingly we start by studying the properties of the function (4.2).

Since small modeling errors and uncertainty are inevitable in a practical design, we wish to characterize the smallest upper bound for the \mathcal{H}_∞ norm of the asymptotic transfer function T_a which is *insensitive* to small delay changes.

DEFINITION 4.2. For $\vec{\tau} \in (\mathbb{R}_0^+)^m$, let the strong \mathcal{H}_∞ norm of T_a , $\|T_a(j\omega, \vec{\tau})\|_\infty$, be defined as

$$\|T_a(j\omega, \vec{\tau})\|_\infty := \lim_{\epsilon \rightarrow 0+} \sup \{ \|T_a(j\omega, \vec{\tau}_\epsilon)\|_\infty : \vec{\tau}_\epsilon \in \mathcal{B}(\vec{\tau}, \epsilon) \cap (\mathbb{R}^+)^m \},$$

Several properties of this upper bound on $\|T_a(j\omega, \vec{\tau})\|_\infty$ are listed below. Recall that Assumption 3.2 is taken.

PROPOSITION 4.3. The following assertions hold:

1. for every $\vec{\tau} \in (\mathbb{R}_0^+)^m$, we have

$$\|T_a(j\omega, \vec{\tau})\|_\infty = \max_{\vec{\theta} \in [0, 2\pi]^m} \sigma_1(\mathbb{T}_a(\vec{\theta})), \quad (4.5)$$

where

$$\mathbb{T}_a(\vec{\theta}) = -CV \left(U^T A_0 V + \sum_{i=1}^m U^T A_i V e^{-j\theta_i} \right)^{-1} U^T B; \quad (4.6)$$

2. $\|T_a(j\omega, \vec{\tau})\|_\infty \geq \|T_a(j\omega, \vec{\tau})\|_\infty$ for all delays $\vec{\tau}$;

3. $\|T_a(j\omega, \vec{\tau})\|_\infty = \|T_a(j\omega, \vec{\tau})\|_\infty$ for rationally independent² $\vec{\tau}$.
Proof. We always have

$$(e^{-j\omega\tau_1}, \dots, e^{-j\omega\tau_m}) \in \{(e^{-j\theta_1}, \dots, e^{-j\theta_m}) : \theta_i \in [0, 2\pi], i = 1, \dots, m\},$$

implying

$$\|T(j\omega, \vec{\tau})\|_\infty \leq \max_{\vec{\theta} \in [0, 2\pi]^m} \sigma_1 \left(\mathbb{T}_a(\vec{\theta}) \right). \quad (4.7)$$

For any $\epsilon > 0$ in Definition 4.2, there exists $\vec{\tau}_\epsilon = [\tau_{\epsilon,1}, \dots, \tau_{\epsilon,m}]$ rationally independent in $\mathcal{B}(\vec{\tau}, \epsilon) \cap (\mathbb{R}^+)^m$. By Theorem 2.1 in [24], given rationally independent time delays $\vec{\tau}_\epsilon$ and for $\vec{\theta} = [\theta_1, \dots, \theta_m]$ arbitrary, there exists a sequence of real numbers $\{\omega_n\}_{n \geq 1}$ such that

$$\lim_{n \rightarrow \infty} \max_{1 \leq i \leq m} |e^{-j\omega_n \tau_{\epsilon,i}} - e^{-j\theta_i}| = 0.$$

It follows that

$$\begin{aligned} \text{closure}\{(e^{-j\omega\tau_{\epsilon,1}}, \dots, e^{-j\omega\tau_{\epsilon,m}}) : \omega \in \mathbb{R}\} = \\ \{(e^{-j\theta_1}, \dots, e^{-j\theta_m}) : \theta_i \in [0, 2\pi], i = 1, \dots, m\}, \end{aligned}$$

implying

$$\|T(j\omega, \vec{\tau}_\epsilon)\|_\infty = \max_{\vec{\theta} \in [0, 2\pi]^m} \sigma_1 \left(\mathbb{T}_a(\vec{\theta}) \right). \quad (4.8)$$

The assertions follow from (4.7) and (4.8). \square

Formula (4.5) in Proposition 4.3 shows that the strong \mathcal{H}_∞ norm of T_a is independent of the delay values. The formula further leads to a computational scheme based on sweeping on $\vec{\theta}$ intervals. This approximation can be corrected by solving a set of nonlinear equations. Numerical computation details are presented in Section 5.1.

We now come back to the properties of the transfer function (4.1) of the system (1.1). As we have illustrated with Example 4.1, a discontinuity of the function (4.2) may carry over to the function (4.1). Therefore, we define the strong \mathcal{H}_∞ norm of the transfer function T in a similar way.

DEFINITION 4.4. For $\vec{\tau} \in (\mathbb{R}_0^+)^m$, the strong \mathcal{H}_∞ norm of T , $\|T(j\omega, \vec{\tau})\|_\infty$, is given by

$$\|T(j\omega, \vec{\tau})\|_\infty := \lim_{\epsilon \rightarrow 0^+} \sup \{ \|T(j\omega, \vec{\tau}_\epsilon)\|_\infty : \vec{\tau}_\epsilon \in \mathcal{B}(\vec{\tau}, \epsilon) \cap (\mathbb{R}^+)^m \}.$$

The following main theorem describes the desirable property that, in contrast to the \mathcal{H}_∞ norm, the strong \mathcal{H}_∞ norm *continuously* depends on the delay parameters. It also presents an explicit expression that lays at the basis of the algorithm to compute the strong \mathcal{H}_∞ norm of a transfer function, presented in the next section. The proof makes use of the technical results in Section A of the Appendix.

²The m components of $\vec{\tau} = (\tau_1, \dots, \tau_m)$ are rationally independent if and only if $\sum_{k=1}^m z_k \tau_k = 0$, $z_k \in \mathbb{Z}$ implies $z_k = 0$, $\forall k = 1, \dots, m$. For instance, two delays τ_1 and τ_2 are rationally independent if their ratio is an irrational number.

THEOREM 4.5. *The strong \mathcal{H}_∞ norm of the transfer function of the DDAE (1.1) satisfies*

$$\| \| T(j\omega, \vec{\tau}) \| \|_\infty = \max(\| T(j\omega, \vec{\tau}) \|_\infty, \| \| T_a(j\omega, \vec{\tau}) \| \|_\infty), \quad (4.9)$$

where T and T_a are the transfer function (3.2) and the asymptotic transfer function (3.4). In addition, the function

$$\vec{\tau} \in (\mathbb{R}_0^+)^m \mapsto \| \| T(j\omega, \vec{\tau}) \| \|_\infty \quad (4.10)$$

is continuous.

Proof. Lemma A.2 implies that the function (4.1) is continuous at delay values where

$$\| T(j\omega, \vec{\tau}) \|_\infty > \| \| T_a(j\omega, \vec{\tau}) \| \|_\infty. \quad (4.11)$$

This property, along with the fact that $\| \| T_a(j\omega, \vec{\tau}) \| \|_\infty$ is independent of $\vec{\tau}$ (see Proposition 4.3), lead to the assertion (4.9) and the continuity of (4.10) under the condition (4.11). In the other case the assertions follow from Lemma A.3. \square

EXAMPLE 4.6. *We come back to Example 4.1. The \mathcal{H}_∞ norm of T , as defined by (4.3), is 2.6422 and the strong \mathcal{H}_∞ norm of the corresponding asymptotic transfer function T_a is 4. From property (4.9), we conclude that the strong \mathcal{H}_∞ norm of T (4.3) is 4.*

REMARK 4.7. *In contrast to delay perturbations, the \mathcal{H}_∞ norm of T is continuous with respect to changes of the system matrices A_i, \dots, A_m, B and C .*

5. Computation of strong H-infinity norms. The algorithm for computing the strong \mathcal{H}_∞ norm of the transfer function of (1.1) is based on property (4.9). Therefore, we first outline in §5.1 the strong \mathcal{H}_∞ norm computation of the asymptotic transfer function T_a , before presenting the algorithm in §5.2.

5.1. Strong H-infinity norm of the asymptotic transfer function. The computation of $\| \| T_a(j\omega, \vec{\tau}) \| \|_\infty$ is based on expression (4.5) in Proposition 4.3. We obtain an approximation by restricting $\vec{\theta}$ in (4.5) to a grid,

$$\| \| T_a(j\omega, \vec{\tau}) \| \|_\infty \approx \max_{\vec{\theta} \in \Theta_h} \sigma_1 \left(\mathbb{T}_a(\vec{\theta}) \right), \quad (5.1)$$

where Θ_h is a m -dimensional grid over the hypercube $[0, 2\pi]^m$ and $\mathbb{T}_a(\vec{\theta})$ is defined by (4.6). If a high accuracy is required, then the approximate results may be corrected by solving the nonlinear equations

$$\begin{cases} \begin{bmatrix} \mathbb{A}_{22}(\vec{\theta}) & -\xi^{-1} B_2 B_2^T \\ \xi^{-1} C_2^T C_2 & -(\mathbb{A}_{22}(\vec{\theta}))^* \end{bmatrix} \begin{bmatrix} u_a \\ v_a \end{bmatrix} = 0, \\ n(u_a, v_a) = 0, \\ \Re(e^{-j\theta_i} (v_a^* A_i^{(22)} u_a)) = 0, \quad i = 1, \dots, m, \end{cases} \quad (5.2)$$

where

$$\mathbb{A}_{22}(\vec{\theta}) = -U^T A_0 V - \sum_{i=1}^m U^T A_i V e^{-j\theta_i} \quad (5.3)$$

and $n(u_a, v_a) = 0$ is a normalization constraint. The first equation in (5.2) implies that ξ is a singular value of $\mathbb{T}_a(\vec{\theta})$. The last equation of (5.2) expresses that the derivatives of the singular value ξ with respect to the elements of $\vec{\theta}$ are zero. In our implementation we solve (5.2) using the Gauss-Newton method, which exhibits quadratic convergence because the (overdetermined) equations have an exact solution, see Section 10.2 of [32].

In most practical problems, the number of delays to be considered in $\mathbb{T}_a(\vec{\theta})$ and $\mathbb{A}_{22}(\vec{\theta})$ is much smaller than the number of system delays, m , because most of the terms in (5.3) are zero. This significantly reduces the computational cost of the sweeping in (5.1). Note that in a control application a nonzero term in (5.3) corresponds to a high frequency feedthrough over the control loop. We illustrate this with the following example.

EXAMPLE 5.1. *Consider the time-delay system*

$$\begin{cases} \dot{x}(t) &= \sum_{i=2}^m M_i x(t - \tau_i) + B_1 w(t), \\ z(t) &= P x(t) + w(t) + N_1 w(t - \tau_1). \end{cases} \quad (5.4)$$

When defining $X = [x^T \gamma_d^T \gamma_w^T]^T$, where γ_d and γ_w are slack variables, the system can be described by equations of the form (1.1) as

$$\left\{ \begin{aligned} \underbrace{\begin{bmatrix} I & 0 & 0 \\ 0 & 0 & 0 \\ 0 & 0 & 0 \end{bmatrix}}_E \dot{X}(t) &= \underbrace{\begin{bmatrix} 0 & 0 & 0 \\ 0 & -I & I \\ 0 & 0 & -I \end{bmatrix}}_{A_0} X(t) + \underbrace{\begin{bmatrix} 0 & 0 & 0 \\ 0 & 0 & N_1 \\ 0 & 0 & 0 \end{bmatrix}}_{A_1} X(t - \tau_1) \\ &+ \sum_{i=2}^m \underbrace{\begin{bmatrix} M_i & 0 & 0 \\ 0 & 0 & 0 \\ 0 & 0 & 0 \end{bmatrix}}_{A_i} X(t - \tau_i) + \underbrace{\begin{bmatrix} B_1 \\ 0 \\ I \end{bmatrix}}_B w(t), \\ z(t) &= \underbrace{\begin{bmatrix} P & I & 0 \end{bmatrix}}_C X(t). \end{aligned} \right.$$

The asymptotic transfer function (3.4) is given by

$$T_a(\lambda) = -CV \left(U^T A_0 V + \sum_{i=1}^m U^T A_i V e^{-\lambda \tau_i} \right)^{-1} U^T B,$$

where $U = V = \begin{pmatrix} 0 & 0 \\ I & 0 \\ 0 & I \end{pmatrix}$. Since $U^T A_i V = 0$ for $i = 2, \dots, m$, $T_a(\lambda)$ reduces to

$$\begin{aligned} T_a(\lambda) &= -CV (U^T A_0 V + U^T A_1 V e^{-\lambda \tau_1})^{-1} U^T B, \\ &= -\begin{bmatrix} I & 0 \end{bmatrix} \begin{bmatrix} -I & -(I + N_1 e^{-\lambda \tau_1}) \\ 0 & -I \end{bmatrix}^{-1} \begin{bmatrix} 0 \\ I \end{bmatrix} \\ &= I + N_1 e^{-\lambda \tau_1}, \end{aligned}$$

which readily follows from (5.4). Although the original system has m delays, the asymptotic transfer function has only one delay τ_1 . Accordingly, the grid Θ_h in the approximation (5.1) reduces to a grid on the interval $[0, 2\pi]$.

In the numerical implementation, we compute the matrix norm of $U^T A_i V$ for $i = 1, \dots, m$ and omit the corresponding time-delays if their norms are less than a tolerance value.

5.2. Algorithm. From (4.9) the following implication can be derived.

$$\|T(j\omega, \vec{\tau})\|_\infty > \|T_a(j\omega, \vec{\tau})\|_\infty \Rightarrow \|T(j\omega, \vec{\tau})\|_\infty = \|T(j\omega, \vec{\tau})\|_\infty.$$

Moreover, we learn from Lemma A.2 that, given a level

$$\xi > \|T_a(j\omega, \vec{\tau})\|_\infty, \quad (5.5)$$

there are only *finitely* many frequencies $\omega \geq 0$ for which a singular value of $T(j\omega, \vec{\tau})$ is equal to ξ . These properties allow an adaptation of the standard level set algorithm for \mathcal{H}_∞ computations for finite-dimensional systems as described in [5]. The differences are two-fold. First one has to restrict to the situation where (5.5) holds. This is possible by a preliminary computation of the strong \mathcal{H}_∞ norm of T_a , as outlined in §5.1, and setting the initial level such that (5.5) is satisfied. Second, the Hamiltonian eigenvalue problem, from which intersections of singular value curves with level sets are computed, is infinite-dimensional, carrying over from the case of retarded time-delay systems discussed in [25]. Therefore, a discretization is necessary, which brings us to a predictor-corrector approach. In the predictor step, an approximation of the strong \mathcal{H}_∞ norm of T (provided it exceeds $\|T_a(j\omega, \vec{\tau})\|_\infty$) is obtained by computing

$$\|T_N(j\omega)\|_\infty$$

using the level set method presented in [5]. Here,

$$T_N(\lambda) := \mathbf{C}_N(\lambda \mathbf{E}_N - \mathbf{A}_N)^{-1} \mathbf{B}_N. \quad (5.6)$$

is the transfer function of the system

$$\begin{cases} \mathbf{E}_N \dot{z}(t) &= \mathbf{A}_N z(t) + \mathbf{B}_N u(t), \\ y(t) &= \mathbf{C}_N z(t), \end{cases}$$

obtained by a spectral discretization of (1.1) on a grid of N points, see Section B of the appendix for the derivation. The correction step serves to remove the discretization error on the result. It is based on solving a system of nonlinear equations that characterize extrema in the singular value curves. The initial conditions are generated in the prediction step, assuring that the algorithm converges to the right peak value. The overall algorithm for the strong \mathcal{H}_∞ norm computation is as follows.

ALGORITHM 5.2.

Input: system data, N , grid Ω_N defined by (B.3), candidate critical frequency $\{\omega_1, \dots, \omega_l\}$ if available, tolerance tol for the prediction step, $\|T_a(j\omega, \vec{\tau})\|_\infty$

1. Prediction step:

(a) *calculate the first level,*

$$\xi_l = \max(\|T_a(j\omega, \vec{\tau})\|_\infty, \sigma_1(T(j\omega_1)), \dots, \sigma_1(T(j\omega_l)))$$

(b) *repeat until break*

i. *set $\xi := \xi_l(1 + 2\text{tol})$*

ii. *compute all $\omega^{(i)} \in \mathbb{R}$ satisfying $\sigma_k(T_N(j\omega^{(i)})) = \xi$. By [17, Proposition 12], this can be done by computing generalized eigenvalues of the pencil*

$$\lambda \begin{bmatrix} \mathbf{E}_N & 0 \\ 0 & \mathbf{E}_N^T \end{bmatrix} - \begin{bmatrix} \mathbf{A}_N & \xi^{-1} \mathbf{B}_N \mathbf{B}_N^T \\ -\xi^{-1} \mathbf{C}_N^T \mathbf{C}_N & -\mathbf{A}_N^T \end{bmatrix}, \quad (5.7)$$

whose imaginary axis eigenvalues are given by $\lambda = j\omega^{(i)}$.

iii. **if** no generalized eigenvalues $j\omega^{(i)}$ of (5.7) exist, **then**

if $\xi_l = |||T_a(j\omega, \vec{\tau})|||_\infty$, **then**

set $|||T(j\omega, \vec{\tau})|||_\infty = |||T_a(j\omega, \vec{\tau})|||_\infty$
quit

else

let $\omega^{(i)} \in \mathbb{R}$ satisfying $\sigma_k(T_N(j\omega^{(i)})) = \xi_l$,
set $\tilde{\xi} = (\xi + \xi_l)/2$, $\tilde{\omega}^{(i)} = \omega^{(i)}$, $i = 1, 2, \dots$
break, go to the correction step 2.

endif

else

calculate $\mu^{(i)} := \sqrt{\omega^{(i)}\omega^{(i+1)}}$, $i = 1, 2, \dots$
set

$$\xi_l := \max_i \max \left(\sigma_1 \left(T_N(j\mu^{(i)}) \right), |||T_a(j\omega, \vec{\tau})|||_\infty \right).$$

endif

2. Correction step:

(a) Solve the nonlinear equations

$$\begin{cases} H(j\omega, \xi) \begin{bmatrix} u \\ v \end{bmatrix} = 0, \\ n(u, v) = 0, \\ \Im\{v^*(E + \sum_{i=1}^m A_i \tau_i e^{-j\omega \tau_i})u\} = 0, \end{cases} \quad (5.8)$$

using the Gauss-Newton method, where

$$H(j\omega, \xi) = \begin{bmatrix} j\omega E - A_0 - \sum_{i=1}^m A_i e^{-j\omega \tau_i} & -\xi^{-1} B B^T \\ \xi^{-1} C^T C & j\omega E^T + A_0^T + \sum_{i=1}^m A_i^T e^{j\omega \tau_i} \end{bmatrix}$$

and $n(u, v) = 0$ is a normalizing condition, with the starting values

$$\omega = \tilde{\omega}^{(i)}, \quad \xi = \tilde{\xi}, \quad \begin{bmatrix} u \\ v \end{bmatrix} = \arg \min \|H(j\tilde{\omega}^{(i)}, \tilde{\xi})\zeta\| / \|\zeta\|;$$

denote the solutions with $(\hat{u}^{(i)}, \hat{v}^{(i)}, \hat{\omega}^{(i)}, \hat{\xi}^{(i)})$, for $i = 1, 2, \dots$,

(b) set $|||T(j\omega)|||_\infty := \max_{1 \leq i \leq p} \hat{\xi}^{(i)}$

The first and the second equation in (5.8) describe the presence of a singular value ξ of matrix $T(j\omega, \vec{\tau})$. The third equation expresses that the derivative of this singular value with respect to ω is equal to zero, see [25]. Hence, Equations (5.8) can be used to correct approximate peak values. Note that the correction step is only performed if

$$|||T(j\omega, \vec{\tau})|||_\infty > |||T_a(j\omega, \vec{\tau})|||_\infty.$$

For details on the choice of the number of discretization points, N , and the tolerance, tol , we refer to [25].

The main ideas behind Algorithm 5.2 are clarified with two examples.

EXAMPLE 5.3.

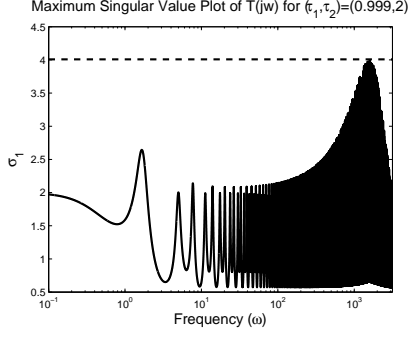


FIG. 5.1. Algorithm 5.2 for the maximum singular value plot of T (4.3): no intersection case.

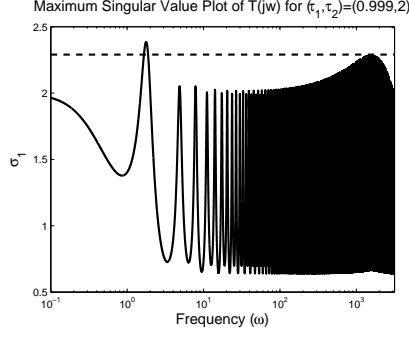


FIG. 5.2. Algorithm 5.2 for the maximum singular value plot of T (5.9): with intersections case.

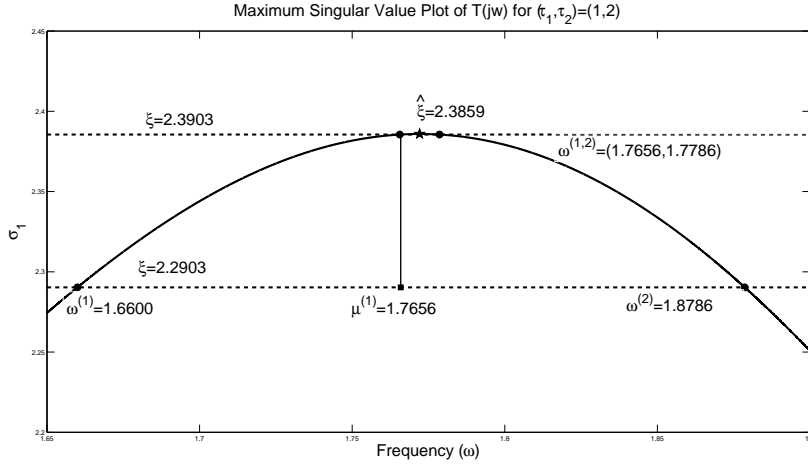


FIG. 5.3. Steps of Algorithm 5.2 for the maximum singular value plot of T (5.9): with intersections case (zoomed).

We apply Algorithm 5.2 to the transfer function T , as specified by (4.3). The strong \mathcal{H}_∞ norm of its asymptotic transfer function T_a (4.4) satisfies $\|T_a(j\omega, \vec{\tau})\|_\infty = 4$. Therefore, the first level is equal to $\xi_l = 4$ in Step (a) of the prediction step of Algorithm 5.2, provided that no candidate frequencies are given. In Step (b) – ii, there is no intersection for the level ξ as shown in Figure 5.1. Therefore the strong \mathcal{H}_∞ norm of T (4.3) is equal to 4 and the correction step is not carried out.

EXAMPLE 5.4. We consider the transfer function

$$T(\lambda, \vec{\tau}) := \frac{\lambda + 2}{\lambda(1 - 1/16e^{-\lambda\tau_1} + 1/2e^{-\lambda\tau_2}) + 1}, \quad (5.9)$$

with $\vec{\tau} = (1, 2)$, and its asymptotic transfer function

$$T_a(\lambda, \vec{\tau}) := \frac{1}{(1 - 1/16e^{-\lambda\tau_1} + 1/2e^{-\lambda\tau_2})}. \quad (5.10)$$

The first level ξ_l in Step (a) is set to the strong \mathcal{H}_∞ norm of T_a (5.10), $\|T_a(j\omega, \vec{\tau})\|_\infty = 2.2857$. In Step (b) – ii, there are two intersections for the level $\xi = 2.2903$, $\omega^{(1)} =$

1.6600 and $\omega^{(2)} = 1.8786$, as shown in Figure 5.2. We can see the details of the next iterations in Figure 5.3. Step (b) – iii calculates the middle frequency $\mu^{(1)} = 1.7656$ and $\xi_l = 2.3855$ for the next level. In the second iteration, the level is set to $\xi = 2.3903$ and the corresponding intersections are $\omega^{(1)} = 1.7656$ and $\omega^{(2)} = 1.7786$. Since there is no intersection in the third iteration due to the chosen tolerance in the prediction step, $\text{tol} = 10^{-3}$, we compute the approximate strong \mathcal{H}_∞ norm of T (5.9) and the frequencies as $\hat{\xi} = 2.3879$ and $(\tilde{\omega}_1, \tilde{\omega}_2) = \{1.7657, 1.7786\}$. In the correction step, these values are corrected and the strong \mathcal{H}_∞ norm of T (5.9) and the corresponding frequency are computed as $\hat{\xi} = 2.3859$ and $\hat{\omega} = 1.7721$.

6. Fixed-Order H-infinity Controller Design. We consider the equations

$$\begin{cases} E\dot{x}(t) = A_0(p)x(t) + \sum_{i=1}^m A_i(p)x(t - \tau_i) + Bw(t), \\ z = Cx(t), \end{cases} \quad (6.1)$$

where the system matrices smoothly depend on parameters p . As illustrated in Section 2, a broad class of interconnected systems can be brought into this form, where the parameters p can be interpreted in terms of a parameterization of a controller. For example, in the feedback interconnection of (2.3) and (2.4) they may correspond to the elements of the matrices of the controller K . Note that, by fixing some elements of these matrices, additional structure can be imposed on the controller, e.g. a proportional-integrative-derivative (PID) like structure.

The proposed method for designing fixed-order/ fixed-structure \mathcal{H}_∞ controllers is based on a direct minimization of the strong \mathcal{H}_∞ norm of the closed-loop transfer function T from w to z as a function of the parameters p . The overall optimization algorithm requires the evaluation of the objective function and its gradients with respect to the optimization parameters, whenever it is differentiable.

The strong \mathcal{H}_∞ norm of the transfer function T can be computed by Algorithm 5.2. The derivatives of the norm with respect to controller parameters exist whenever there are unique values $\vec{\tau}$ or $\vec{\theta}$ such that

$$\|T(j\omega, \vec{\tau})\|_\infty = \hat{\xi} = \begin{cases} \sigma_1 \left(\mathbb{T}_a \left(\vec{\theta} \right) \right), & \text{if } \hat{\xi} = \|T_a \left(\vec{\theta}, \vec{\tau} \right)\|_\infty, \\ \sigma_1(T(j\hat{\omega})), & \text{if } \hat{\xi} > \|T_a \left(\vec{\theta}, \vec{\tau} \right)\|_\infty, \end{cases}$$

holds and, in addition, the largest singular value $\hat{\xi}$ has multiplicity one. We compute the derivative of the strong \mathcal{H}_∞ norm of T with respect to the parameter p_k as

$$\frac{\partial \hat{\xi}}{\partial p_k} = \begin{cases} -2\hat{\xi}^2 \frac{\Re \left(v_a^* \frac{\partial A_{22}(\vec{\theta})}{\partial p_k} u_a \right)}{v_a^* B_2 B_2^T v_a + u_a^* C_2^T C_2 u_a} \Big|_{(\xi, \vec{\theta}) = (\hat{\xi}, \vec{\theta})} & \text{if } \hat{\xi} = \|T_a \left(\vec{\theta}, \vec{\tau} \right)\|_\infty, \\ -2\hat{\xi}^2 \frac{\Re \left(v^* \frac{\partial A(j\hat{\omega})}{\partial p_k} u \right)}{v^* B B^T v + u^* C^T C u} \Big|_{(\xi, \omega) = (\hat{\xi}, \hat{\omega})} & \text{if } \hat{\xi} > \|T_a \left(\vec{\theta}, \vec{\tau} \right)\|_\infty, \end{cases}$$

where given $\xi = \hat{\xi}$, u_a, v_a and u, v are vectors in (5.2) and (5.8) for $\vec{\theta} = \vec{\theta}$ and $\omega = \hat{\omega}$ respectively. For more details on the computation of derivatives we refer to [31, 18].

The overall design procedure is fully automated and does not require any interaction with the user. The computation cost of the optimization algorithm is dominated by the evaluation of the strong \mathcal{H}_∞ norm of the closed-loop transfer function T for the parameters p at each iteration. The first main part in this computation is to find

the strong \mathcal{H}_∞ norm of the asymptotic transfer function by computing the maximum singular value of \mathbb{T}_a at $p_a^{m_a-1}$ points spanning the grid Θ_h in (5.1), where p_a is the number of grid points in the interval $[0, 2\pi]$ (the default value is 20 in our implementation) and m_a is the number of actual delays appearing in $\mathbb{A}_{22}(\vec{\theta})$, see (5.3). Note that the number of delays m_a is usually much smaller than the number of system delays, see the arguments at the end of §5.1. Therefore the computational cost for sweeping is usually not very high. It is even completely skipped if there is no high frequency feedthrough in the control loop (which results in $m_a = 0$). The second main part is the computation of the generalized eigenvalues of the pencil (5.7) in the prediction step of Algorithm 5.2. This computation requires solving a generalized eigenvalue problem with dimensions $2nN$ where the default value for N is 20 in our implementation. The number of iteration steps of the optimization algorithm heavily depends on the optimization problem under consideration. In most cases, satisfactory results are already obtained in the first phase of the optimization algorithm where the BFGS algorithm is used. For the behavior of BFGS, applied to nonsmooth problems, we refer to [22].

Recall that the feedback interconnection of system (2.3) and controller (2.4) can be rewritten in the form (6.1) in such a way that the closed-loop matrices depend affinely on the matrices of the controller. This property improves the performance of the optimization method. Note that in the existing work for systems without delay (see, e.g., [20]) the dependency is in general nonlinear, due to the use of elimination for handling a non-trivial feedthrough, as illustrated in Example 2.1.

7. Examples. In §7.1 we illustrate some aspects of the proposed approach on two motivating examples. In §7.2 apply the approach to benchmark examples collected from the literature. In §7.3 we consider 5 additional problems.

7.1. Motivating Examples. As a first example we consider a plant with the state-space representation

$$\dot{x}(t) = -x(t) - 0.5x(t-1) + w(t) + u(t-0.2), \quad z(t) = x(t) + u(t-0.2), \quad y(t) = x(t),$$

and a controller $u(t) = Ky(t)$. The closed-loop transfer function can be written as

$$T(s) = \frac{1 + Ke^{-0.2s}}{s + 1 - Ke^{-0.2s} + 0.5e^{-s}}. \quad (7.1)$$

The closed-loop system is internally stable for $-7.9 < K < 1.5$. As illustrated in Figure 7.1, the closed-loop system achieves the minimum strong \mathcal{H}_∞ norm $\hat{\xi}$ for $K = -0.8813$. The iterations of the optimization method (starting at $K = -7.4$ and shown in circles) converge to the minimum, 0.2137.

The second example concerns the design of a static controller for the case where the standard \mathcal{H}_∞ norm and the strong \mathcal{H}_∞ norm of the closed-loop systems are different. The transfer function T , as defined by (4.3), can be interpreted as the transfer function of the closed-loop system formed by the plant

$$\begin{cases} \begin{bmatrix} 1 & 0 \\ 0 & 0 \end{bmatrix} \dot{x}(t) &= \begin{bmatrix} -0.1 & -1 \\ 1 & -1 \end{bmatrix} x(t) + \begin{bmatrix} 0 \\ 1 \end{bmatrix} u(t) + \begin{bmatrix} 0 \\ 1 \end{bmatrix} w(t), \\ z(t) &= \begin{bmatrix} 2 & -1 \end{bmatrix} x(t), \\ y(t) &= \begin{bmatrix} 0 & 1 \\ 0 & 0 \end{bmatrix} x(t - \tau_1) + \begin{bmatrix} 0 & 0 \\ 0 & 1 \end{bmatrix} x(t - \tau_2), \end{cases}$$

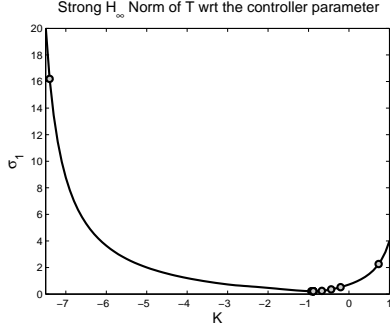


FIG. 7.1. The strong \mathcal{H}_∞ norm of T (7.1) with respect to the controller parameter.

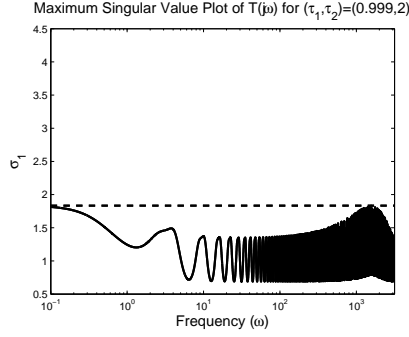


FIG. 7.2. The maximum singular value plot of the closed-loop system $T(j\omega)$ (4.3) for $(\tau_1, \tau_2) = (0.999, 2)$ with the controller K_{opt} .

where $(\tau_1, \tau_2) = (1, 2)$ and the controller

$$u(t) = Ky(t),$$

where $K = K_{init} = \begin{bmatrix} 0.25 & -0.5 \end{bmatrix}$. In Example 5.3, we computed the standard \mathcal{H}_∞ norm 2.5788 and the strong \mathcal{H}_∞ norm 4, as illustrated in Figure 5.1 with slightly perturbed delay values. An optimization of the strong \mathcal{H}_∞ norm results in

$$K = K_{opt} = \begin{bmatrix} -0.3533 & -0.1012 \end{bmatrix}$$

and the corresponding optimal value is given by 1.8333. As shown in Figure 7.2, the optimization method pushes the strong \mathcal{H}_∞ norm of the asymptotic transfer function until it is equal to the standard \mathcal{H}_∞ norm. Hence, the minimum is characterized by a balance between low and high frequency behavior of the transfer function.

7.2. A collection of examples from the literature. We collected benchmark examples for \mathcal{H}_∞ optimization of time-delay systems from the literature. We considered two types of problems: the \mathcal{H}_∞ optimization with *state* and *output* feedback controllers. Our results are given in Table 7.1 and 7.2 respectively.

Problem	Other Methods	Results	Computed Controller
Ex. 4, [14]	1.8822, [10]	0.1000	$[-2.3273, -9.5004 \cdot 10^3]$
	0.2284, [13]		
	0.1287, [14]		
Ex. 1, [12]	0.4215, [12]	0.4005	$[-17.8065, 9.5915]$
Ex. 2, [15]	21, [15]	2.9091	$[-1.1151 \cdot 10^3, -1.6189 \cdot 10^4]$

TABLE 7.1
The achieved \mathcal{H}_∞ performances by state-feedback controllers

The strong \mathcal{H}_∞ norm of the closed-loop system in Example 4 of [14] with respect to controller parameters is visualized in Figure 7.3. The closed-loop system is stable for sufficiently large negative K_2 and its norm converges to 0.1 as $K_2 \rightarrow -\infty$, for any value of K_1 . This is confirmed by the property that all suggested controllers in the literature have large negative K_2 values. The starting point $K = [0, -5]$ and

other points are shown as a red dot and gray dots respectively in Figure 7.3. The iterations of the optimization method get closer to the value 0.1 for large negative values of K_2 without a significant change in the K_1 parameter. Note that there is no finite minimum and the algorithm stops when the number of iterations exceeds the maximum number of iterations in the algorithm. By analyzing similar plots as in Figure 7.3, we confirmed that the optimization method reaches close to optimal values for the other two examples in Table 7.1. Note that Example 2 concerns a DDAE while the others concern retarded time-delay systems.

The strong \mathcal{H}_∞ norm of the closed-loop system in Example 4 of [14] with respect to controller parameters is given in Figure 7.3. The closed-loop system is stable for sufficiently large negative K_2 and its norm converges to 0.1, for any value of K_1 . This is confirmed by the property that all suggested controllers in the literature have large negative K_2 values. The starting point $K = [0, -5]$ and other points are shown as a red dot and gray dots respectively in Figure 7.3. The iterations of the optimization method get closer to the value 0.1 for large negative values of K_2 without a significant change in the K_1 parameter. By analyzing similar plots as in Figure 7.3, we confirmed that the optimization method reaches close to optimal values for the other two examples in Table 7.1. Note that Example 2 concerns a DDAE while the others concern retarded time-delay systems.

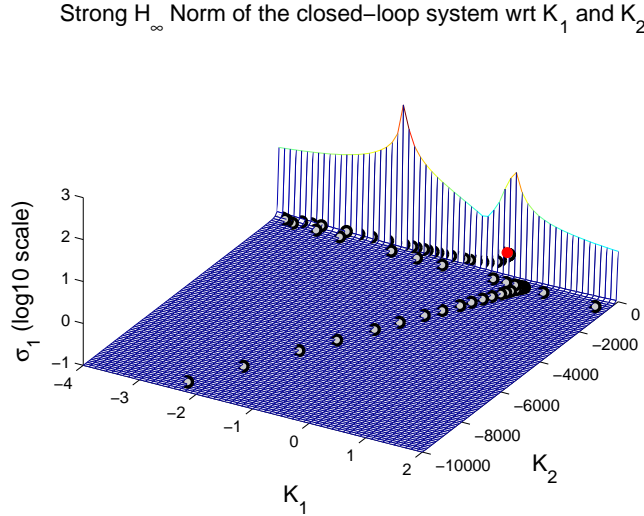


FIG. 7.3. The strong \mathcal{H}_∞ norm of the closed-loop system in Example 4 [14] with respect to controller parameters, $K = [K_1 \ K_2]$.

The designed controllers for the examples in Table 7.2 have a state-feedback-observer structure. The observer is a time-delay system and estimates the states of the original plant. Example 3 is described by a DDAE and Example 4 is a retarded time-delay system. The strong \mathcal{H}_∞ norms of the closed-loop system in Example 4 of [15] for $h = 0.999$ and $h = 1.28$ with respect to controller parameters are given in Figure 7.4 and 7.5. The optimal controller gain does not change for two different delays. In both cases, the optimization method reaches the optimal value.

In [27] the robust stabilization of a time-delay system of retarded type by a static state-feedback controller is addressed. This problem is formulated as a \mathcal{H}_∞ synthesis problem. The approximate \mathcal{H}_∞ norm is computed using a frequency grid.

Problem	Other Methods	Results	Computed Controller
Ex. 3, [15]	2.4, [15]	3.7654	$[-8.6961]$
		1.2618	$\begin{bmatrix} -7.1827 & -37.3389 \\ 18.6767 & 90.4893 \end{bmatrix}$
		1.2428	$\begin{bmatrix} -2.6837 & -15.1028 & -6.2101 \\ 0.3607 & 1.2086 & 3.6959 \\ 0.1379 & -3.9720 & 10.4548 \end{bmatrix}$
Ex. 4, [15] ($h = 0.999$)	0.8600, [14] 11, [15]	0.1617	$[-16.1692]$
Ex. 4, [15] ($h = 1.28$)	20, [15]	0.1617	$[-16.1692]$

TABLE 7.2
The achieved \mathcal{H}_∞ performances by output-feedback controllers

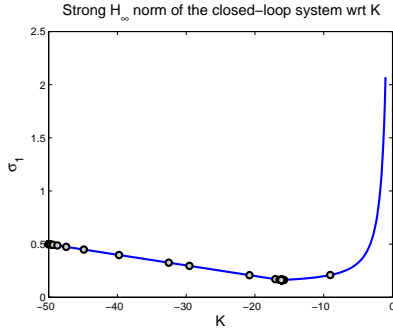


FIG. 7.4. The strong \mathcal{H}_∞ norm of the closed-loop system in Example 4 ($h = 0.999$) [15] with respect to the controller parameter.

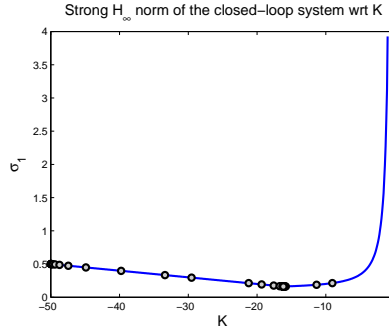


FIG. 7.5. The strong \mathcal{H}_∞ norm of the closed-loop system in Example 4 ($h = 1.28$) [15] with respect to the controller parameter.

The minimization is performed by a continuation approach where the highest peak values in the singular value plot are monitored. We applied our method on the numerical problem in Section 5 of this reference and obtained a similar result. The optimized \mathcal{H}_∞ norm is 3.3145 and the corresponding state-feedback controller is given by

$$K = \begin{bmatrix} 0.7763 & 1.1119 & 0.5433 \end{bmatrix}.$$

In [29] a state-feedback controller is designed for time-delay systems based on quasi-direct pole placement. This approach allows to assign a number of fixed right-most poles while shifting the remaining part of the spectrum as far to the left as possible. We designed a static \mathcal{H}_∞ controller for the experimental heat transfer set-up described in Section 3 of [29]. This is an 11th-order retarded time-delay system with 5 state delays and 1 input delay,

$$\begin{cases} \dot{x}(t) = A_0 x(t) + \sum_{i=1}^5 A_i x(t - \tau_i) + w(t) + B u(t - \tau_6), \\ z(t) = x(t), \quad y(t) = x(t) \end{cases}$$

where system matrices and delays, A_0 , A_i and τ_i for $i = 0, \dots, 5$ are given in [29]. The

performance channels are set to identity matrices. The controller parameters of four static controllers designed using quasi-direct pole-placement are given in Table 1 of [29]. The closed-loop strong \mathcal{H}_∞ norms with these controllers are 779.1600, 1881.3944, 1155.7140, 2113.8085. We achieved a minimal closed-loop strong \mathcal{H}_∞ norm 386.3491 by a static \mathcal{H}_∞ controller, $u(t) = Kx(t)$, where

$$K = \begin{bmatrix} -1.3414 & -5.7544 & 1.0440 & 0.5181 & -29.9649 & -5.0182 \\ -12.4284 & 0.6694 & 4.7125 & -23.6380 & 2.3902 \end{bmatrix}.$$

Finally, in [18] a direct optimization approach is applied to the design of fixed-order \mathcal{H}_∞ controllers for a class of retarded time-delay systems where the controller has no feedthrough term. The second example in [18] is a 4th-order time-delay system with 4 delays. The system is stable and its \mathcal{H}_∞ norm is 1.3907. In Table 7.3, we present our results for different controller orders n_K for this example, without any additional restriction on the controller.

n_K	Results	Computed Controller			
1	1.2513	-0.3068	0.9590		
		0.0166	0.0186		
2	1.2508	-0.0959	-0.0624	-0.0982	
		-0.0024	-0.1984	0.0883	
		-0.0756	0.0347	0.0234	
3	1.2493	-0.0861	-0.0673	-0.0953	-0.0519
		0.0046	-0.2170	-0.0233	0.1083
		-0.0016	0.0010	-0.2973	0.1995
		-0.1734	-0.1040	-0.0475	0.0362

TABLE 7.3

The achieved \mathcal{H}_∞ performances for the time-delay system in [18] by dynamic controllers

7.3. Benchmark results. In Table 7.4, we present the results of benchmarking of our code with 5 additional problems. The plants are retarded time-delay systems of the form (2.3). The second column shows the size of matrices A_i , n , and the total number of time-delays in the plant, m . The third column gives order n_K of the (finite-dimensional) controller. The first line for each plant displays the closed-loop strong \mathcal{H}_∞ norm when there is no controller (excepting the fourth plant which is unstable). The fourth and fifth columns contain the optimized strong \mathcal{H}_∞ norm of the closed-loop system and the corresponding controller.

The problem data for the above benchmark examples and a MATLAB implementation of our code for the strong \mathcal{H}_∞ controller design are available at the website <http://twr.cs.kuleuven.be/research/software/delay-control/hinfopt/>.

8. Conclusions. We considered the fixed-order/fixed-structure \mathcal{H}_∞ controller design problem for delay differential algebraic systems. The main contributions are as follows.

1. We show that a very broad class of interconnected systems can be brought in the standard form (1.1) in a systematic way. Input/output delays and direct feedthrough terms can be dealt with by introducing slack variables. The dependence of the closed-loop matrices on the controller parameters always remains linear.

Plants	(n,m)	n_K	Results	Computed Controller
#1	(2,2)	—	44.7086	—
		0	5.1499	[−2.8858]
		1	5.1037	$\begin{bmatrix} -3.8529 & 1.4636 \\ -1.8703 & -2.0389 \end{bmatrix}$
		2	5.1029	$\begin{bmatrix} -4.6132 & 6.5495 & -2.2860 \\ -3.1847 & -4.7981 & 2.4295 \\ -3.9177 & 1.0307 & -2.7309 \end{bmatrix}$
#2	(3,5)	—	17.3595	—
		0	1.9604	[0.0641]
		1	1.9004	$\begin{bmatrix} -0.1140 & 1.9984 \\ -0.0083 & 0.0626 \end{bmatrix}$
		2	1.8695	$\begin{bmatrix} -0.4458 & -0.0416 & 1.9645 \\ -0.4998 & -0.4274 & 0.9799 \\ -0.0223 & 0.0125 & 0.0653 \end{bmatrix}$
#3	(4,7)	—	22.5669	—
		0	7.9522	$\begin{bmatrix} -0.4435 \\ -2.5784 \end{bmatrix}$
		1	7.9220	$\begin{bmatrix} -2.3222 & 0.3329 \\ 0.5662 & -0.4290 \\ -0.9636 & -2.5278 \end{bmatrix}$
		2	7.9071	$\begin{bmatrix} -2.3261 & 0.3181 & 0.2772 \\ -0.7214 & -1.4068 & 0.1320 \\ 0.5882 & -0.2219 & -0.4312 \\ -0.9382 & 0.3012 & -2.5353 \end{bmatrix}$
#4	(6,2)	0	165.0013	[−2]
		0	0.4199	[−3778.5600]
		1	0.2275	$\begin{bmatrix} -121.3792 & -1.4191 \\ -27.6931 & -13.8822 \end{bmatrix}$
		2	0.1081	$\begin{bmatrix} -2.3590 & 9.2505 & -11.2683 \\ -1.5130 & -3.6363 & 5.8830 \\ -5.9382 & 7.9907 & -23.7252 \end{bmatrix}$
#5	(8,6)	—	1.4291	—
		0	0.4751	[−1.9792]
		1	0.2818	$\begin{bmatrix} -1.3299 & 1.2660 \\ -6.1379 & -1.0250 \end{bmatrix}$
		2	0.2809	$\begin{bmatrix} -1.7327 & 1.9221 & -4.0733 \\ -2.6273 & -2.0103 & -2.7046 \\ 2.6669 & -3.2341 & -1.4181 \end{bmatrix}$

TABLE 7.4
The achieved \mathcal{H}_∞ performances for benchmark problems

2. We demonstrated the sensitivity of the \mathcal{H}_∞ norm w.r.t. small delay perturbations and introduced the *strong* \mathcal{H}_∞ norm for DDAEs, inline with the notion of strong stability, and we analyzed its properties.
3. We presented a predictor-corrector algorithm for the (strong) \mathcal{H}_∞ norm computation of DDAEs.
4. Based on the numerical algorithm for the strong \mathcal{H}_∞ norm and its gradient

computation with respect to controller parameters, we applied non-smooth, non-convex optimization methods for designing controllers with a fixed order or structure.

The presented approach has been validated by numerical examples. An implementation of the algorithms is available from

<http://twr.cs.kuleuven.be/research/software/delay-control/hinfopt/>.

Acknowledgements. This article presents results of the Belgian Programme on Interuniversity Poles of Attraction, initiated by the Belgian State, Prime Ministers Office for Science, Technology and Culture, of the Optimization in Engineering Centre OPTEC, and of the project STRT1-09/33 of the K.U.Leuven Research Council.

REFERENCES

- [1] S. Boyd and V. Balakrishnan. A regularity result for the singular values of a transfer matrix and a quadratically convergent algorithm for computing its \mathcal{L}_∞ -norm. *Systems & Control Letters*, 15:1–7, 1990.
- [2] S. Boyd, V. Balakrishnan, and P. Kabamba. A bisection method for computing the \mathcal{H}_∞ norm of a transfer matrix and related problems. *Mathematics of Control, Signals and Systems*, 2:207–219, 1989.
- [3] D. Breda, S. Maset, and R. Vermiglio. Pseudospectral differencing methods for characteristic roots of delay differential equations. *SIAM Journal on Scientific Computing*, 27(2):482–495, 2005.
- [4] D. Breda, S. Maset, and R. Vermiglio. Pseudospectral approximation of eigenvalues of derivative operators with non-local boundary conditions. *Applied Numerical Mathematics*, 56:318–331, 2006.
- [5] N.A. Bruinsma and M. Steinbuch. A fast algorithm to compute the \mathcal{H}_∞ -norm of a transfer function matrix. *Systems and Control Letters*, 14:287–293, 1990.
- [6] J. V. Burke, D. Henrion, A. S. Lewis, and M. L. Overton. HIFOO - a MATLAB package for fixed-order controller design and H-infinity optimization. In *Proceedings of the 5th IFAC Symposium on Robust Control Design*, Toulouse, France, 2006.
- [7] R. Byers. A bisection method for measuring the distance of a stable matrix to the unstable matrices. *SIAM Journal on Scientific and Statistical Computing*, 9(9):875–881, 1988.
- [8] R.F. Curtain and H. Zwart. *An introduction to infinite-dimensional linear systems theory*, volume 21 of *Texts in Applied Mathematics*. Springer-Verlag, 1995.
- [9] J.C. Doyle, K. Glover, Khargonekar P.P., and Francis B.A. State-space solutions to standard \mathcal{H}^2 and \mathcal{H}^∞ control problems. *IEEE Transactions on Automatic Control*, 34(8):831–847, 1989.
- [10] E. Fridman. New Lyapunov-Krasovskii functionals for stability of linear retarded and neutral type systems. *Systems & Control Letters*, 43(4):309–319, 2001.
- [11] E. Fridman. Stability of linear descriptor systems with delay: a lyapunov-based approach. *Journal of Mathematical Analysis and Applications*, 273:24–44, 2002.
- [12] E. Fridman and U. Shaked. \mathcal{H}_∞ -state-feedback control of linear systems with small state delay. *Systems & Control Letters*, 33:141–150, 1998.
- [13] E. Fridman and U. Shaked. New bounded real lemma representations for time-delay systems and their applications. *IEEE Trans. Autom. Control*, 46:1973–1979, 2001.
- [14] E. Fridman and U. Shaked. A descriptor system approach to H_∞ control of linear time-delay systems. *IEEE Trans. Autom. Control*, 47(2):253–270, 2002.
- [15] E. Fridman and U. Shaked. H_∞ -control of linear state-delay descriptor systems: an LMI approach. *Linear Algebra and its Applications*, 351-352:271–302, 2002.
- [16] P. Gahinet and P. Apkarian. A linear matrix inequality approach to \mathcal{H}_∞ control. *International Journal of Robust and Nonlinear Control*, 4(4):421–448, 1994.
- [17] Y. Genin, R. Stefan, and P. Van Dooren. Real and complex stability radii of polynomial matrices. *Linear Algebra and its Applications*, 351-352:381–410, 2002.
- [18] S. Gumussoy and W. Michiels. Fixed-order H-infinity optimization of time-delay systems. In M. Diehl, F. Glineur, E. Jarlebring, and W. Michiels, editors, *Recent Advances in Optimization and its Applications in Engineering*. Springer, 2010.
- [19] S. Gumussoy and W. Michiels. A predictor-corrector type algorithm for the pseudospectral abscissa computation of time-delay systems. *Automatica*, 46(4):657–664, 2010.

- [20] S. Gumussoy and M.L. Overton. Fixed-order H-infinity controller design via HIFOO, a specialized nonsmooth optimization package. In *Proceedings of the American Control Conference*, pages 2750–2754, Seattle, USA, 2008.
- [21] J.K. Hale and S.M. Verduyn Lunel. Strong stabilization of neutral functional differential equations. *IMA Journal of Mathematical Control and Information*, 19:5–23, 2002.
- [22] A. Lewis and M.L. Overton. Nonsmooth optimization via BFGS. Available from <http://cs.nyu.edu/overton/papers.html>, 2009.
- [23] H. Logemann. Destabilizing effects of small time-delays on feedback-controlled descriptor systems. *Linear Algebra and its Applications*, 272:131–153, 1998.
- [24] W. Michiels, K. Engelborghs, D. Roose, and D. Dochain. Sensitivity to infinitesimal delays in neutral equations. *SIAM Journal on Control and Optimization*, 40(4):1134–1158, 2002.
- [25] W. Michiels and S. Gumussoy. Characterization and computation of H-infinity norms of time-delay systems. *SIAM Journal on Matrix Analysis and Applications*, 31(4):2093–2115, 2010.
- [26] W. Michiels and S.-I. Niculescu. *Stability and stabilization of time-delay systems. An eigenvalue based approach*. SIAM, 2007.
- [27] W. Michiels and D. Roose. An eigenvalue based approach for the robust stabilization of linear time-delay systems. *International Journal of Control*, 76(7):678–686, 2003.
- [28] W. Michiels and T. Vyhldal. An eigenvalue based approach for the stabilization of linear time-delay systems of neutral type. *Automatica*, 41(6):991–998, 2005.
- [29] W. Michiels, T. Vyhldal, and P. Zitek. Control for time-delay systems based on quasi-direct pole placement. *Journal of Process Control*, 20(3):337–343, 2010.
- [30] W. Michiels, T. Vyhldal, P. Zitek, H. Nijmeijer, and D. Henrion. Strong stability of neutral equations with an arbitrary delay dependency structure. *SIAM Journal on Control and Optimization*, 48(2):763–786, 2009.
- [31] Millstone, M. HIFOO 1.5: Structured control of linear systems with a non-trivial feedthrough. Master’s thesis, New York University, 2006.
- [32] J. Nocedal and S.J. Wright. *Numerical Optimization*. Springer Series in Operations Research. Springer, 1999.
- [33] M. Overton. HANSO: a hybrid algorithm for nonsmooth optimization. Available from <http://cs.nyu.edu/overton/software/hanso/>, 2009.
- [34] T. Stykel. On criteria for asymptotic stability of differential algebraic equations. *ZAMM Z. Angew. Math. Mech.*, 82(3):147–158, 2002.
- [35] K. Zhou, J.C. Doyle, and K. Glover. *Robust and optimal control*. Prentice Hall, 1995.

Appendix A. Some technical lemmas.

LEMMA A.1. *For all $\gamma > 0$, there exist numbers $\epsilon > 0$ and $\Omega > 0$ such that*

$$\sigma_1(T(j\omega, \vec{r}) - T_a(j\omega, \vec{r})) < \gamma$$

for all $\omega > \Omega$ and $\vec{r} \in \mathcal{B}(\vec{r}, \epsilon) \cap (\mathbb{R}^+)^m$.

Proof. The uniformity of the bound γ w.r.t. small delay perturbations stems from the fact that the bound (3.5) is a continuous function of the delays \vec{r} at their nominal values. The latter is implied by the *strong* stability assumption (Assumption 3.2). \square

LEMMA A.2. *Let $\xi > \|T_a(j\omega, \vec{r})\|_\infty$ hold. Then there exist real numbers $\epsilon > 0$, $\Omega > 0$ and an integer N such that for any $\vec{r} \in \mathcal{B}(\vec{r}, \epsilon) \cap (\mathbb{R}^+)^m$, the number of frequencies $\omega^{(i)}$ such that*

$$\sigma_k(T(j\omega^{(i)}, \vec{r})) = \xi, \tag{A.1}$$

for some $k \in \{1, \dots, n\}$, is smaller than N , and, moreover, $|\omega^{(i)}| < \Omega$.

Proof. For any (fixed) value of $\xi > 0$ and delays \vec{r} , the relation

$$\sigma_k(T(j\omega), \vec{r}) = \xi \tag{A.2}$$

holds for some $\omega \in \mathbb{R}$ and $k \in \{1, \dots, n\}$ if and only if $\lambda = j\omega$ is a zero of the function

$$\det \left(\begin{bmatrix} \lambda E - A_0 - \sum_{i=1}^m A_i e^{-\lambda r_i} & -\frac{1}{\xi} B B^T \\ \frac{1}{\xi} C C^T & \lambda E^T + A_0^T + \sum_{i=1}^m A_i^T e^{\lambda r_i} \end{bmatrix} \right). \tag{A.3}$$

This result is a variant of Lemma 2.1 of [25] to which we refer for the proof.

Now take $\xi > \|T_a(j\omega, \vec{\tau})\|_\infty$. From Lemma A.1, and taking into account that $\|T_a(j\omega, \vec{\tau})\|_\infty$ does not depend on $\vec{\tau}$ (see Proposition 4.3) it follows that there exists numbers $\epsilon > 0$ and $\Omega > 0$ such that all ω satisfying (A.2) for some $k \in \{1, \dots, n\}$ and $\vec{r} \in \mathcal{B}(\vec{\tau}, \epsilon) \cap (\mathbb{R}^+)^m$ also satisfy $|\omega| < \Omega$. This proves one statement. At the same time $\lambda = j\omega$ must be a zero of the analytic function (A.3). The other statement is due to the fact that an analytic function only has finitely many zeros in a compact set. \square

LEMMA A.3. *The following implication holds*

$$\|T(j\omega, \vec{\tau})\|_\infty \leq \|T_a(j\omega, \vec{\tau})\|_\infty \Rightarrow \|T(j\omega, \vec{\tau})\|_\infty = \|T_a(j\omega, \vec{\tau})\|_\infty.$$

Proof. For every $\epsilon > 0$ there exist delays $\vec{\tau}_0$ and a frequency ω_0 such that

$$\|\vec{\tau}_0 - \vec{\tau}\| < \epsilon/2, \quad \sigma_1(T_a(j\omega_0, \vec{\tau}_0)) \geq \|T_a(j\omega, \vec{\tau})\|_\infty - \epsilon/2.$$

In addition, there exist commensurate delays

$$\vec{\tau}_r = \left(\frac{n_1}{s}, \dots, \frac{n_m}{s} \right), \quad (\text{A.4})$$

with $(n_1, \dots, n_m, s) \in \mathbb{N}^{m+1}$ such that

$$\|\vec{\tau}_r - \vec{\tau}_0\| < \epsilon/2, \quad |\sigma_1(T_a(j\omega_0, \vec{\tau}_r)) - \sigma_1(T_a(j\omega_0, \vec{\tau}_0))| \leq \epsilon/2.$$

Thus, for all $\epsilon > 0$ there exist commensurate delays (A.4) and a frequency ω_0 satisfying

$$\|\vec{\tau}_r - \vec{\tau}\| < \epsilon, \quad \sigma_1(T_a(j\omega_0, \vec{\tau}_r)) \geq \|T_a(j\omega, \vec{\tau})\|_\infty - \epsilon.$$

From the fact that

$$T_a(j\omega_0, \vec{\tau}_r) = T_a(j(\omega_0 + 2\pi sk), \vec{\tau}_r)$$

for all $k \geq 1$ and Lemma A.1, we conclude that

$$\|T(j\omega, \vec{\tau})\|_\infty \geq \|T_a(j\omega, \vec{\tau})\|_\infty. \quad (\text{A.5})$$

Now take a level $\xi > \|T_a(j\omega, \vec{\tau})\|_\infty$, and let ϵ and Ω be determined by the assertion of Lemma A.2. From the assumption $\|T(j\omega, \vec{\tau})\|_\infty \leq \|T_a(j\omega, \vec{\tau})\|_\infty$ and the relation between (A.2) and (A.3) it follows that the function (A.3) has no zeros on the imaginary axis for $\vec{r} = \vec{\tau}$. Because the function (A.3) is analytic and all potential imaginary axis zeros have modulus smaller than Ω whenever $\vec{r} \in \mathcal{B}(\vec{\tau}, \epsilon) \cap (\mathbb{R}^+)^m$, we conclude that there exists a number $\epsilon_2 > 0$ such that the function (A.3) has no imaginary axis eigenvalues whenever $\vec{r} \in \mathcal{B}(\vec{\tau}, \epsilon_2) \cap (\mathbb{R}^+)^m$. Equivalently, $T(j\omega, \vec{r})$ has no singular values equal to ξ whenever $\vec{r} \in \mathcal{B}(\vec{\tau}, \epsilon_2) \cap (\mathbb{R}^+)^m$. This proves that the left and the right hand side of (A.5) are equal. \square

Appendix B. Finite dimensional approximation.

We start by reformulating the system (1.1) as an infinite-dimensional linear system, inspired by [8]. When defining the Hilbert space $X := \mathbb{C}^n \times \mathcal{L}_2([-\tau_{\max}, 0], \mathbb{C}^n)$ equipped with the inner product

$$\langle (y_0, y_1), (z_0, z_1) \rangle_X = \langle y_0, z_0 \rangle_{\mathbb{C}^n} + \langle y_1, z_1 \rangle_{\mathcal{L}_2},$$

where $\tau_{\max} := \max(\tau_1, \dots, \tau_m)$, we can rewrite (1.1) as

$$\begin{aligned}\mathcal{E}\dot{z}(t) &= \mathcal{A}z(t) + \mathcal{B}u(t), \\ y(t) &= \mathcal{C}z(t),\end{aligned}\tag{B.1}$$

where

$$\begin{aligned}\mathcal{D}(\mathcal{A}) &= \{z = (z_1, z_0) \in X : z_1 \text{ is absolutely continuous} \\ &\quad \text{on } [-\tau_{\max}, 0], \frac{dz_1}{d\theta} \in \mathcal{C}([-\tau_{\max}, 0], \mathbb{C}^n), z_0 = z_1(0)\},\end{aligned}\tag{B.2}$$

$$\begin{aligned}\mathcal{E}z &= \begin{pmatrix} z_1 \\ Ez_0 \end{pmatrix}, \quad \mathcal{A}z = \begin{pmatrix} \frac{dz_1}{d\theta}(\cdot) \\ A_0z_0 + \sum_{i=1}^m A_i z_1(-\tau_i) \end{pmatrix}, z \in \mathcal{D}(\mathcal{A}), \\ \mathcal{B}u &= \begin{pmatrix} 0 \\ Bu \end{pmatrix}, u \in \mathbb{C}^{n \times n_u}, \quad \mathcal{C}z = Cz_0, z \in X.\end{aligned}$$

The connection between (1.1) and (B.1) is that $z_0(t) \equiv x(t)$, $z_1(t) \equiv x(t + \theta)$, $\theta \in [-\tau_{\max}, 0]$.

Next, we discretize the infinite-dimensional system (B.1). We use a spectral method, as in [3, 4]. Given a positive integer N , we consider a mesh Ω_N of $N + 1$ distinct points in the interval $[-\tau_{\max}, 0]$,

$$\Omega_N = \{\theta_{N,i}, i = -N, \dots, 0\},\tag{B.3}$$

where we assume that $\theta_{N,0} = 0$. With the Lagrange polynomials $l_{N,k}$ defined as real valued polynomials of degree N satisfying

$$l_{N,k}(\theta_{N,i}) = \begin{cases} 1 & i = k \\ 0 & i \neq k \end{cases}$$

for $i, k \in \{-N, \dots, 0\}$, we can, similarly as in [3], approximate (B.1) and, hence, (1.1), by the finite-dimensional system:

$$\mathbf{E}_N \dot{z}(t) = \mathbf{A}_N z(t) + \mathbf{B}_N u(t), \quad z(t) \in \mathbb{R}^{(N+1)n \times 1}\tag{B.4}$$

$$y(t) = \mathbf{C}_N z(t)\tag{B.5}$$

where

$$\mathbf{A}_N = \begin{bmatrix} d_{-N,-N}I_n & \dots & d_{-N,-1}I_n & d_{-N,0}I_n \\ \vdots & & \vdots & \vdots \\ d_{-1,-N}I_n & \dots & d_{-1,-1}I_n & d_{-1,0}I_n \\ \Gamma_{-N} & \dots & \Gamma_{-1} & \Gamma_0 \end{bmatrix}, \quad \mathbf{B}_N = \begin{bmatrix} 0 \\ \vdots \\ 0 \\ B \end{bmatrix}\tag{B.6}$$

$$\mathbf{E}_N = \begin{bmatrix} I_{nN} & 0_{nN \times n} \\ 0_{n \times nN} & E \end{bmatrix}, \quad \mathbf{C}_N = [0 \quad \dots \quad 0 \quad C]\tag{B.7}$$

and

$$\begin{aligned}\Gamma_0 &= A_0 + \sum_{l=1}^m A_l l_{N,0}(-\tau_l), \\ \Gamma_k &= \sum_{l=1}^m A_l l_{N,k}(-\tau_l), \quad k \in \{-N, \dots, -1\}, \\ d_{i,k} &= l'_{N,k}(\theta_{N,i}), \quad i, k \in \{-N, \dots, 0\}.\end{aligned}$$

The transfer function of (B.4) is given by (5.6). Using the arguments as spelled out in [19, 25] it can be shown that the effect of the approximation of (3.2) by (5.6) can be interpreted as the effect of approximating the exponential functions in (3.2) by rational functions. This interpretation can be used to estimate the frequency interval where the main peaks in the singular value plot occur (see [25, §4.3]).

Appendix C. Numerical data in Section 7.2. The state-space equations of the numerical examples in Section 7.2 are as follows.

C.1. Example 4 in [14].

$$\begin{aligned}\dot{x}_1(t) &= -x_1(t - 0.999) - x_2(t - 0.999) + w(t), \\ \dot{x}_2(t) &= x_2(t) - 0.9x_2(t - 0.999) + w(t) + u(t), \\ z_1(t) &= x_2(t), \quad z_2(t) = 0.1u(t), \quad y_1(t) = x_1(t), \quad y_2(t) = x_2(t).\end{aligned}$$

C.2. Example 1 in [12].

$$\begin{aligned}\dot{x}_1(t) &= 2x_1(t) + x_2(t) - x_1(t - 0.1) - 0.5w(t) + 3u(t), \\ \dot{x}_2(t) &= -x_2(t) - x_1(t - 0.1) + x_2(t - 0.1) + w(t) + u(t), \\ z_1(t) &= x_1(t) - 0.5x_2(t), \quad z_2(t) = u(t), \quad y_1(t) = x_1(t), \quad y_2(t) = x_2(t).\end{aligned}$$

C.3. Example 2 in [15].

$$\begin{aligned}\dot{x}_1(t) &= -x_1(t - 1.2) + w(t) - 0.5u(t), \quad 0 = x_1(t - 1.2) - x_2(t - 1.2) + w(t) + u(t), \\ z_1(t) &= x_1(t) + 0.2x_2(t) + 0.1u(t), \quad y_1(t) = x_1(t), \quad y_2(t) = x_2(t).\end{aligned}$$

C.4. Example 3 in [15].

$$\begin{aligned}\dot{x}_1(t) &= -x_1(t - 1.2) + w_1(t), \quad 0 = x_2(t) + x_1(t - 1.2) - x_2(t - 1.2) + w_1(t) + u(t), \\ z_1(t) &= x_1(t) + 0.2x_2(t) + 0.1u(t), \quad y_1(t) = x_1(t) + 0.1w_2(t).\end{aligned}$$

C.5. Example 4 in [15].

$$\begin{aligned}\dot{x}_1(t) &= -x_1(t - h) - x_2(t - h) + w_1(t), \quad \dot{x}_2(t) = x_2(t) - 0.9x_2(t - h) + w_1(t) + u(t), \\ z_1(t) &= x_2(t), \quad z_2(t) = 0.1u(t), \quad y_1(t) = x_2(t) + 0.1w_2(t).\end{aligned}$$

C.6. Example in [27].

$$\dot{x}(t) = Ax(t) + Bw(t) + Bu(t - 5), \quad z(t) = I_3x(t), \quad y(t) = I_3x(t)$$

where

$$A = \begin{pmatrix} -0.08 & -0.03 & 0.2 \\ 0.2 & -0.04 & -0.005 \\ -0.06 & 0.2 & -0.07 \end{pmatrix}, \quad B = \begin{pmatrix} -0.1 \\ -0.2 \\ 0.1 \end{pmatrix}.$$

C.7. Example in [29].

$$\dot{x}(t) = A_0 + \sum_{i=1}^5 A_i x(t - h_i) + I_{11}w(t) + Bu(t - 7), \quad z(t) = I_{11}x(t), \quad y(t) = I_{11}x(t)$$

where the time-delays are $h_1 = 3$, $h_2 = 5$, $h_3 = 15$, $h_4 = 23$, $h_5 = 29$. The system matrices A_i for $i = 0, \dots, 6$ are real-valued 11×11 matrices. The (k, l)

non-zero element of A_i th matrix is denoted by $A_i^{(k,l)}$ and the numerical values are $A_0^{(1,1),(3,3),(5,5),(9,9)} = -0.2$, $A_0^{(4,7),(4,8),(8,3),(8,4)} = 0.1417$, $A_0^{(2,2)} = -0.04$, $A_0^{(6,6)} = -0.0588$, $A_0^{(6,6)} = -1$, $A_0^{(10,10)} = -0.0667$, $A_0^{(4,3)} = A_0^{8,7} = 0.1917$, $A_0^{(4,4)} = A_0^{(8,8)} = -0.04$, $A_1^{(5,4)} = 0.195$, $A_2^{(3,2)} = 0.1966$, $A_2^{(6,5)} = 0.0529$, $A_2^{(9,8)} = 0.194$, $A_2^{(10,9)} = 0.0613$, $A_3^{1,6} = 0.1946$, $A_4^{2,1} = 0.0384$, $A_5^{7,7} = -0.0159$.

C.8. Example 2 in [18].

$$\begin{aligned} \dot{x}(t) &= \begin{pmatrix} -4.4656 & -0.4271 & 0.4427 & -0.1854 \\ -0.8601 & -5.6257 & 0.8577 & -0.5210 \\ 0.9001 & -0.7177 & -6.5358 & 0.0417 \\ -0.6836 & 0.0242 & 0.4997 & -3.5618 \end{pmatrix} x(t) + \begin{pmatrix} 0.6848 & -0.0618 & 0.5399 & 0.5057 \\ 0.3259 & -0.3810 & 0.6592 & -0.0066 \\ 0.6325 & 0.3752 & 0.4122 & 0.7303 \\ 0.5878 & 0.9737 & 0.1907 & -0.8639 \end{pmatrix} \\ &+ \begin{pmatrix} 0.9371 & -0.7859 & 0.1332 & 0.7429 \\ -0.8025 & 0.4483 & 0.6226 & 0.0152 \\ 0.0940 & 0.2274 & 0.1536 & 0.5776 \\ -0.1941 & 0.5659 & 0.8881 & -0.0539 \end{pmatrix} x(t-3.2) + \begin{pmatrix} 1 & 0 \\ -1.6 & 1 \\ 0 & 0 \\ 0 & 0 \end{pmatrix} w(t) \\ &+ \begin{pmatrix} 0.6576 & -0.8543 & -0.3460 & 0.6415 \\ -0.3550 & 0.5024 & 0.6081 & 0.9038 \\ 0.9523 & 0.6624 & 0.0765 & -0.8475 \\ -0.4436 & 0.8447 & -0.0734 & 0.4173 \end{pmatrix} x(t-3.9) + \begin{pmatrix} 0.2 \\ -1 \\ 0.1 \\ -0.4 \end{pmatrix} u(t-0.2) \\ z(t) &= \begin{pmatrix} 1 & 0 & 0 & -1 \\ 0 & -1 & 1 & 0 \end{pmatrix} x(t) + \begin{pmatrix} 0.1 & 1 \\ -1 & 0.2 \end{pmatrix} w(t) + \begin{pmatrix} 1 \\ -1 \end{pmatrix} u(t) \\ y(t) &= \begin{pmatrix} 1 & 0 & -1 & 0 \end{pmatrix} x(t) + \begin{pmatrix} -2 & 0.1 \end{pmatrix} w(t) + 0.4u(t-0.2) \end{aligned}$$